JCTC Journal of Chemical Theory and Computation

Article

pubs.acs.org/JCTC

Investigating the Effects of Basis Set on Metal–Metal and Metal–Ligand Bond Distances in Stable Transition Metal Carbonyls: Performance of Correlation Consistent Basis Sets with 35 Density Functionals

Beulah S. Narendrapurapu, Nancy A. Richardson, Andreas V. Copan, Marissa L. Estep, Zheyue Yang, and Henry F. Schaefer, III*

Center for Computational Quantum Chemistry, University of Georgia, Athens, Georgia

Supporting Information

ABSTRACT: Density functional theory (DFT) is a widely used method for predicting equilibrium geometries of organometallic compounds involving transition metals, with a wide choice of functional and basis set combinations. A study of the role of basis set size in predicting the structural parameters can be insightful with respect to the effectiveness of using small basis sets to optimize larger molecular systems. For many organometallic systems, the metal–metal and metal–carbon distances are the most important structural features. In this study, we compare the equilibrium metal–ligand and metal–metal distances of six transition metal carbonyl compounds predicted by the Hood-Pitzer double-ζ polarization (DZP) basis set, against those predicted employing the standard correlation consistent cc-pVXZ (X = D,T,Q) basis sets, for 35 different DFT methods. The effects of systematically increasing the basis set size on the structural parameters are carefully investigated. The Mn–Mn bond distance in $Mn_2(CO)_{10}$ shows a greater dependence on basis set size compared to the other M–M bonds. However, the DZP predictions for r_e(Mn–Mn) are closer to experiment than those obtained with the much larger cc-pVQZ basis set. Our results show that, in general, DZP basis sets predict structural parameters with an accuracy comparable to the triple and quadruple-ζ basis sets. This finding is very significant, because the quadruple-ζ basis set for $Mn_2(CO)_{10}$ includes 1308 basis functions, while the equally effective double-ζ set (DZP) includes only 366 basis functions. Overall, the DZP M06-L method predicts structures that are very consistent with experiment.

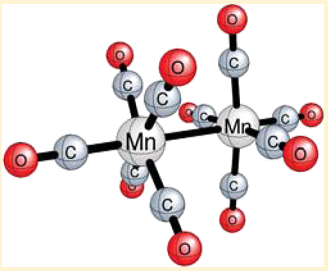

1. INTRODUCTION

Density Functional Theory (DFT) has become a method of choice for predicting the molecular properties of large molecular systems, especially those that contain transition metals.[1] Systems that contain transition metal atoms often exhibit degenerate or near degenerate electronic states, rendering it challenging to systematically include large amounts of multireference character in wave function based methods. Apart from this, DFT competes well in accuracy, for most systems, with simple wave function based methods. The cost-effectiveness of DFT renders it a very practical method for computing the properties of very large systems. In the past few decades, the equilibrium geometries of many transition metal organometallic compounds and metal clusters have been obtained using DFT. In cases where crystallographic information is not yet available, DFT structures are typically the only ones known. The DFT computed structures and vibrational frequencies of a number of homoleptic binuclear metal carbonyl compounds have been reported in the past.[2] The metal–metal and metal–carbon bond distances in these compounds were often computed using standard double-ζ plus polarization (DZP) basis sets. A critical structural feature of the binuclear transition metal compounds is the metal–metal bond, especially multiple bonds in case of unsaturated metal carbonyls. Though not infallible, the metal–metal bond distance is an indicator for direct metal–metal interactions in these compounds.

DFT offers a wide choice of functional and basis set combinations for modeling the structures of organometallic compounds involving metal–metal bonds. Functionals that are calibrated for main group elements are to be used with caution for transition metal compounds. Recent studies have focused on benchmarking functionals that are suitable for computing various transition metal properties. In regard to metal–metal and metal–ligand bond lengths, Zhao and Truhlar examined the performance of 57 functionals with double and triple-ζ basis sets and suggested G96LYP, MPWLYP1M, XLYP, BLYP, MOHLYP, and mPWLYP as functionals of best choice.[3,4] In their 2003 assessment of the role of basis sets in density functional theory, Handy et al. suggested that basis sets of triple-ζ quality are preferable over basis sets of double-ζ quality.[5] Previous studies have suggested that Dunning basis sets are not an optimal choice for density functional computations,[6] yet there are many studies which use Dunning basis sets in the literature. Very recently (2013), Jensen proposed polarization consistent basis sets optimized for density functional calculations for the transition metals Sc–

Received: February 18, 2013

   dx.doi.org/10.1021/ct4002398 | J. Chem. Theory Comput. XXXX, XXX, XXX–XXX

Zn.[9] In relation to the behavior of correlation consistent basis sets in DFT, Wilson and co-workers tested six commonly used functionals with cc-pVxZ (x = D, T, Q, 5) basis sets to predict the molecular properties of first-row closed shell molecules and observed a convergence in molecular properties with increasing basis set size.[7] In another related study, Cundari, Wilson, and co-workers indicated increased accuracies for enthalpies of formation for transition metal carbonyls upon increasing the basis set size from cc-pVTZ to cc-pVQZ for generalized gradient exchange (GGE), hybrid GGA (HGGA), and hybrid meta-GGA (HMGGA) functionals.[8]

In this study, we have performed full geometry optimizations on six transition metal carbonyl compounds, three of which are bimetallic. We studied the changes in metal−metal (M−M) and metal−carbon bond parameter with increasing basis set size from double to triple and quadruple-ζ basis sets and for 35 different density functionals. Although many structure vs basis set studies have been reported for DFT, no such systematic study for organometallics appears in the literature.

2. METHODS

Four basis sets were chosen for this study. The first is an extension of the Dunning double-ζ plus polarization (DZP) basis, and the others are the standard Dunning-Balabanov-Peterson correlation consistent cc-pVXZ (X = D, T, Q) basis sets.[10−12] The Dunning's DZP basis sets for C and O have one set of pure spherical harmonic d-functions with orbital components α_d(C) = 0.75 and α_d(O) =0.85 in addition to Dunning's standard double-ζ (DZ) contraction[13] of Huzinaga's primitive sets[14] and are designated (9s5p1d/4s2p1d). The extended DZP basis sets for transition metals, designated (14s11p6d/10s8p3d), are constructed from Watcher's primitive sets[15] augmented by two sets of p functions and one set of d functions and contracted following Hood and Pitzer.[16] The computations reported here are all-electron, nonrelativistic in nature.

Geometries of all six transition metal carbonyls were optimized using the NWChem6.1 package.[17] The dependence of metal−metal bond distances on basis set was tested for 35 functionals: five generalized gradient approximation (GGA) functionals, two meta GGA functionals, seventeen hybrid GGA functionals, nine hybrid meta GGAs, and two long-range correlated hybrid meta GGAs. Since the M05-2X method and the M06 suite of functionals are sensitive to the choice of quadrature grid, the NWChem fine integration grid with (140, 974) points for the five 3d transition metals and (70, 590) points for C and O was chosen.[18] The grid employs the Mura-Knowles[19] radial quadrature and Lebedev angular quadrature[20] and was used for all DFT methods. All geometries were optimized employing the NWChem 'tight' convergence option with an SCF convergence of 10^{-8}.

3. RESULTS AND DISCUSSION

Metal−carbon (M−C) and metal−metal (M−M) bond distances for the six carbonyl compounds, computed by the 35 functionals using the four basis sets, are reported in Tables 1−6 and compared with the available experimental structures. The tables consist of functionals grouped according to their type and arranged in decreasing order of the Hartree−Fock contribution to the DFT method within each group, wherever applicable. The functionals we have chosen in this study predict geometries that are reasonably close to the experimental structures. We have computed the mean absolute deviation (MAD) of each bond length by averaging over the absolute deviations (from experimental values) of bond lengths obtained from the four basis sets. For all molecules other than $Mn_2(CO)_{10}$, fewer than five functionals yield M−M and M−C bond distances with MADs greater than 0.05 Å (see Tables S1a−S6a in the Supporting Information). Almost all the functionals predict M−C bond distances with greater consistency than M−M bond lengths. Overall, the M06-L functional performs the best in predicting molecular geometries, with the exception of the bond between Co and the bridging carbon which is overestimated by ∼0.022 Å compared to the experimental bond distance.[21] The primary focus of our

Table 1. $Ni(CO)_4$ Bond Distances in Angstroms

DFT method	DZP Ni−C	cc-pVDZ Ni−C	cc-pVTZ Ni−C	cc-pVQZ Ni−C
GGA				
BLYP	1.847	1.853	1.853	1.852
BP86	1.826	1.829	1.829	1.827
B97-D	1.843	1.847	1.845	1.845
HCTH147	1.833	1.836	1.834	1.833
HCTH407	1.831	1.833	1.832	1.831
Meta GGA				
M06-L	1.838	1.839	1.836	1.835
VSXC	1.859	1.863	1.861	1.860
Hybrid GGA				
BHLYP	1.848	1.854	1.853	1.852
MPW1K	1.823	1.826	1.825	1.824
BHandH	1.832	1.837	1.836	1.835
MPW1PW91	1.823	1.826	1.824	1.824
MPW1PBE	1.821	1.824	1.822	1.821
B1LYP	1.846	1.851	1.851	1.850
PBE1PBE	1.821	1.824	1.823	1.822
MPW1LYP	1.844	1.850	1.850	1.849
B98	1.837	1.841	1.840	1.839
X3LYP	1.840	1.845	1.845	1.844
B97-1	1.838	1.841	1.841	1.840
B97-2	1.831	1.834	1.833	1.832
MPW3PBE	1.821	1.825	1.824	1.823
B3LYP	1.841	1.846	1.846	1.845
B3PW91	1.824	1.827	1.826	1.825
B3P86	1.820	1.823	1.822	1.821
O3LYP	1.831	1.834	1.833	1.832
Hybrid Meta GGA				
M06-HF	1.929	1.930	1.926	1.928
M05-2X	1.871	1.877	1.876	1.875
M06-2X	1.899	1.906	1.905	1.905
MPWB1K	1.827	1.830	1.829	1.828
BB1K	1.828	1.831	1.830	1.829
M05	1.845	1.850	1.851	1.848
B1B95	1.827	1.830	1.829	1.828
M06	1.844	1.850	1.851	1.849
TPSSH	1.827	1.830	1.828	1.827
LC Hybrid GGA				
CAM-B3LYP	1.831	1.836	1.837	1.836
LC-ωPBE[d]	1.817	1.819	1.819	1.818
experiment-1[a]	1.838	1.838	1.838	1.838
experiment-2[b]	1.84	1.84	1.84	1.84
experiment-3[c]	1.817	1.817	1.817	1.817

[a]Reference 24, gas ED structure. [b]Reference 22, crystal structure. [c]Reference 23, crystal structure. [d]cam 0.3 cam_alpha 0.00 cam_beta 1.00 parameters are used to define the functional (see ref 83).

dx.doi.org/10.1021/ct4002398 | J. Chem. Theory Comput. XXXX, XXX, XXX−XXX

Table 2. $Fe(CO)_5$ Bond Distances in Angstroms

	DZP		cc-pVDZ		cc-pVTZ		cc-pVQZ	
DFT method	$Fe-C^{ax}$	$Fe-C^{eq}$	$Fe-C^{ax}$	$Fe-C^{eq}$	$Fe-C^{ax}$	$Fe-C^{eq}$	$Fe-C^{ax}$	$Fe-C^{eq}$
GGA								
BLYP	1.826	1.827	1.834	1.833	1.831	1.832	1.831	1.832
BP86	1.805	1.805	1.811	1.810	1.809	1.809	1.808	1.809
B97-D	1.812	1.812	1.818	1.817	1.815	1.816	1.814	1.816
HCTH147	1.799	1.801	1.805	1.805	1.802	1.804	1.801	1.804
HCTH407	1.794	1.796	1.800	1.801	1.797	1.800	1.796	1.799
Meta GGA								
M06-L	1.816	1.813	1.820	1.816	1.816	1.812	1.815	1.812
VSXC	1.835	1.835	1.841	1.839	1.838	1.837	1.837	1.837
Hybrid GGA								
BHLYP	1.854	1.822	1.865	1.829	1.859	1.827	1.859	1.827
MPW1K	1.812	1.794	1.819	1.798	1.814	1.797	1.814	1.797
BHandH	1.830	1.806	1.839	1.811	1.834	1.810	1.833	1.809
MPW1PW91	1.803	1.795	1.809	1.800	1.806	1.798	1.806	1.798
MPW1PBE	1.801	1.793	1.807	1.797	1.804	1.796	1.803	1.796
B1LYP	1.830	1.820	1.839	1.827	1.836	1.825	1.835	1.825
PBE1PBE	1.801	1.793	1.806	1.797	1.803	1.796	1.803	1.796
MPW1LYP	1.829	1.819	1.838	1.826	1.835	1.825	1.834	1.824
B98	1.816	1.809	1.823	1.814	1.819	1.812	1.819	1.812
X3LYP	1.823	1.815	1.831	1.821	1.828	1.820	1.827	1.820
B97-1	1.816	1.810	1.824	1.815	1.820	1.813	1.819	1.813
B97-2	1.805	1.799	1.811	1.804	1.807	1.802	1.807	1.802
MPW3PBE	1.801	1.795	1.807	1.800	1.804	1.798	1.803	1.798
B3LYP	1.823	1.816	1.831	1.822	1.828	1.821	1.827	1.821
B3PW91	1.803	1.797	1.809	1.802	1.806	1.800	1.806	1.800
B3P86	1.800	1.794	1.806	1.799	1.803	1.798	1.802	1.797
O3LYP	1.800	1.798	1.805	1.802	1.802	1.801	1.802	1.800
Hybrid Meta GGA								
M06-HF	1.964	1.849	1.992	1.860	1.960	1.845	1.961	1.840
M05-2X	1.853	1.824	1.865	1.831	1.855	1.825	1.854	1.824
M06-2X	1.883	1.840	1.898	1.848	1.882	1.839	1.881	1.838
MPWB1K	1.814	1.796	1.821	1.800	1.818	1.800	1.817	1.799
BB1K	1.813	1.797	1.821	1.801	1.817	1.800	1.816	1.800
M05	1.808	1.811	1.813	1.815	1.811	1.815	1.809	1.813
B1B95	1.806	1.797	1.812	1.801	1.809	1.801	1.809	1.801
M06	1.816	1.816	1.821	1.820	1.822	1.822	1.821	1.821
TPSSH	1.810	1.806	1.816	1.810	1.813	1.808	1.812	1.808
LC Hybrid GGA								
CAM-B3LYP	1.815	1.806	1.824	1.812	1.821	1.812	1.820	1.811
LC-ωPBE[d]	1.791	1.789	1.797	1.794	1.795	1.794	1.794	1.793
experiment-1[a]	1.807	1.827	1.807	1.827	1.807	1.827	1.807	1.827
experiment-2[b]	1.810	1.842	1.810	1.842	1.810	1.842	1.810	1.842
experiment-3[c]	1.811	1.803	1.811	1.803	1.811	1.803	1.811	1.803

[a]Reference 32, gas ED structure. [b]Reference 33, gas ED structure. [c]Reference 23, crystal structure. [d]Refer to Table 1 footnote.

study is to investigate the role of increasing basis set size on the convergence of structural parameters. Tables 1 −6 compare optimized bond parameters across the four basis sets for various DFT functionals. We have also provided tables to compare the predicted structures with experiment (see Tables S1a−S6a). Also reported are comparisons of bond distances from cc-pVXZ (X = D,T,Q) basis sets to the DZP results (see Tables S1b−S6b in the Supporting Information).

A. $Ni(CO)_4$. Solid state and gaseous state structures of the well-known tetrahedral $Ni(CO)_4$ molecule have been determined in the past by X-ray diffraction[22,23] and electron diffraction (ED) experiments.[24] The geometry of $NiCO)_4$ was previously optimized by a number of DFT methods which determined the bond parameters with reasonable accuracy.[25−27] Table 1 shows the variation of M−C bond lengths with increasing basis set size. The computed bond lengths are in good agreement with the experimental values. All four basis sets predict similar structural parameters with differences in M−C bond lengths ranging from lower than 0.001 Å to 0.007 Å across the basis sets. Increasing the size of correlation consistent basis sets from the double-ζ to the triple- and quadruple-ζ has no significant effect on the M−C bond distances; the differences are as small as 0.002 Å. The bond lengths increase slightly, with a mean value of 0.003 Å, from DZP to cc-pVDZ basis and contract by about the same amount upon approaching cc-pVQZ basis.

B. $Fe(CO)_5$. $Fe(CO)_5$ is a trigonal bipyramidal molecule with D_{3h} symmetry and two different M−C distances representing

dx.doi.org/10.1021/ct4002398 | J. Chem. Theory Comput. XXXX, XXX, XXX−XXX

Table 3. $Cr(CO)_6$ Bond Distances in Angstroms

DFT method	DZP Cr−C	cc-pVDZ Cr−C	cc-pVTZ Cr−C	cc-pVQZ Cr−C
GGA				
BLYP	1.931	1.931	1.934	1.934
BP86	1.907	1.905	1.908	1.909
B97-D	1.919	1.917	1.921	1.921
HCTH147	1.903	1.901	1.905	1.905
HCTH407	1.898	1.897	1.900	1.900
Meta GGA				
M06-L	1.922	1.919	1.919	1.921
VSXC	1.946	1.943	1.946	1.946
Hybrid GGA				
BHLYP	1.933	1.933	1.935	1.935
MPW1K	1.900	1.897	1.900	1.901
BHandH	1.915	1.913	1.916	1.916
MPW1PW91	1.900	1.897	1.900	1.901
MPW1PBE	1.897	1.895	1.898	1.898
B1LYP	1.928	1.928	1.931	1.931
PBE1PBE	1.897	1.895	1.897	1.898
MPW1LYP	1.927	1.927	1.930	1.930
B98	1.913	1.913	1.914	1.915
X3LYP	1.922	1.922	1.925	1.925
B97-1	1.914	1.913	1.915	1.915
B97-2	1.904	1.901	1.904	1.905
MPW3PBE	1.899	1.897	1.900	1.900
B3LYP	1.923	1.923	1.925	1.925
B3PW91	1.901	1.899	1.902	1.903
B3P86	1.898	1.896	1.899	1.900
O3LYP	1.900	1.898	1.901	1.901
Hybrid Meta GGA				
M06-HF	1.950	1.954	1.943	1.940
M05-2X	1.929	1.928	1.928	1.929
M06-2X	1.945	1.944	1.942	1.942
MPWB1K	1.902	1.899	1.903	1.903
BB1K	1.902	1.899	1.903	1.904
M05	1.910	1.907	1.910	1.910
B1B95	1.901	1.899	1.903	1.904
M06	1.915	1.913	1.918	1.919
TPSSH	1.911	1.909	1.911	1.912
LC Hybrid GGA				
CAM-B3LYP	1.913	1.912	1.916	1.917
LC-ωPBE[d]	1.891	1.887	1.892	1.893
experiment-1[a]	1.914	1.914	1.914	1.914
experiment-2[b]	1.909	1.909	1.909	1.909
experiment-3[c]	1.915	1.915	1.915	1.915

[a]Reference 47, neutron diffraction. [b]Reference 48, crystal structure. [c]Reference49, crystal structure (higher order X-ray data). [d]Refer to Table 1 footnote.

the axial ($Fe-C^{ax}$) and equatorial ($Fe-C^{eq}$) bonds. There is some experimental uncertainty regarding the relative lengths of the axial and equatorial Fe−C bonds. Gas phase electron diffraction studies[23,28−33] predict shorter $Fe-C^{ax}$ bonds compared to $Fe-C^{eq}$, whereas the X-ray diffraction study of the crystal[23] suggests an opposite trend. Theoretical studies, both ab initio[34−36] and DFT,[35−39] gave divided results about the relative axial and equatorial Fe−C bond distances. Fe−C distances obtained from the density functional methods employed in this study are well within 0.05 Å of the gas electron diffraction experiment.[32] Except for the pure GGA functionals and the M05 hybrid meta GGA, all functionals employed in our study predict slightly longer axial than

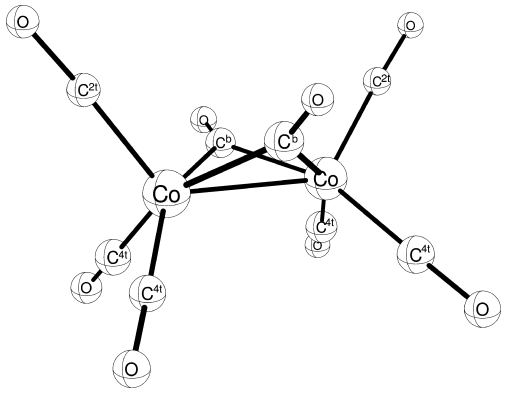

Figure 1. $Co_2(CO)_8$ - C_{2v} symmetry.

equatorial bonds. The axial bonds are shorter than the equatorial bonds by ∼0.003 Å in the case of pure GGAs and the M05 functional. The $Fe-C^{ax}$ bonds are longer than the $Fe-C^{eq}$ by ∼0.008 Å for most hybrid and hybrid meta GGAs, and this trend is consistent with the solid state experimental results. For methods with more than 40% Hartree−Fock contribution, the axial Fe−C bond lengths are significantly longer than Fe−C equatorial bond lengths (∼0.031 Å and ∼0.012 Å for BHLYP and M06-HF, respectively).

Table 2 shows the variation of $Fe-C^{ax}$ and $Fe-C^{eq}$ bonds with increasing basis set size. For most of the methods, the correlation consistent basis sets predict slightly longer Fe−C bonds compared to those from the DZP basis set. Fe−C bond lengths converge at the cc-pVTZ basis set and do not seem to differ by any more than 0.001 with further increase in basis set size. Both $Fe-C^{ax}$ and $Fe-C^{eq}$ elongate by an average distance of 0.004 with increase in basis set size from DZP to cc-pVTZ basis, with the exception of M06-HF functional, where bond distances decrease with increase in basis set size.

C. $Cr(CO)_6$. Structure of the octahedral Cr(CO)6 molecule had been studied theoretically[40−46] by a number of density functional methods, and the agreement with experimental results[47−49] has been demonstrated in the past. The Cr−C bond distance (see Table 3) is reasonably independent of the basis set size for the functionals considered in this study. In all the mononuclear carbonyl compounds considered in this study, the DZP basis set performs exceptionally well in predicting M−C bond distances on par with the cc-pVQZ basis set results. The cc-pVDZ and cc-pVTZ basis sets also perform well.

D. $Co_2(CO)_8$. $Co_2(CO)_8$ is a very important highly fluxional molecule. In solution, the dibridged C_{2v} structure (see Figure 1) exists in equilibrium with the nonbridged D_{3d} structure, and a D_{2d} nonbridged structure has also been suggested by experiments.[50−53] Out of the three structures, the C_{2v} structure is lowest in energy.[54] In the present study, we have optimized the dibridged structure whose crystal structure is well-known[21,55,56] and is used to compare M−M bond lengths in various theoretical studies.[57−65] The Co−Co and Co−C bond differences are presented in Table 4. The B97-2, M06-L, and M06 functionals predict Co−Co and the two terminal Co−C bond distances within 0.010 Å of experimental values with all four basis sets, the differences being least in the case of the DZP basis set, but in the case of the bridging $Co-C^b$, the M06-L functional overestimates the bond distance by ∼0.022 Å.

The structural parameters between DZP and cc-pVXZ (X = D,T,Q) basis sets differ much more in $Co_2(CO)_8$ than in the mononuclear transition metal carbonyls, and the difference is

dx.doi.org/10.1021/ct4002398 | J. Chem. Theory Comput. XXXX, XXX, XXX−XXX

Table 4. $Co_2(CO)_8$ Bond Distances in Angstroms

	DZP				cc-pVDZ				cc-pVTZ				cc-pVQZ			
DFT method	Co−Co	Co−C[b]	Co−C[2t]	Co−C[4t]	Co−Co	Co−C[b]	Co−C[2t]	Co−C[4t]	Co−Co	Co−C[b]	Co−C[2t]	Co−C[4t]	Co−Co	Co−C[b]	Co−C[2t]	Co−C[4t]
GGA																
BLYP	2.599	1.982	1.828	1.835	2.606	1.986	1.833	1.841	2.605	1.987	1.834	1.840				
BP86	2.550	1.957	1.805	1.813	2.556	1.961	1.809	1.818	2.553	1.960	1.808	1.815				
B97-D	2.548	1.969	1.821	1.824	2.555	1.973	1.825	1.829	2.552	1.972	1.824	1.827				
HCTH147	2.554	1.957	1.806	1.812	2.562	1.960	1.810	1.817	2.558	1.959	1.809	1.814	2.561	1.958	1.809	1.813
HCTH407	2.545	1.952	1.802	1.808	2.554	1.955	1.806	1.812	2.548	1.953	1.805	1.808	2.551	1.953	1.805	1.808
Meta GGA																
M06-L	2.525	1.961	1.815	1.825	2.536	1.962	1.818	1.829	2.527	1.960	1.815	1.822	2.526	1.960	1.813	1.822
VSXC	2.496	1.990	1.841	1.859	2.499	1.986	1.845	1.863	2.496	1.988	1.844	1.861				
Hybrid GGA																
BHLYP	2.533	1.940	1.828	1.839	2.546	1.946	1.833	1.844	2.545	1.947	1.833	1.841	2.548	1.947	1.834	1.841
MPW1K	2.487	1.919	1.798	1.807	2.495	1.923	1.801	1.811	2.493	1.923	1.800	1.807	2.496	1.923	1.801	1.807
BHandH	2.504	1.926	1.809	1.819	2.515	1.931	1.813	1.824	2.513	1.931	1.813	1.821	2.516	1.931	1.813	1.820
MPW1PW91	2.507	1.932	1.798	1.806	2.514	1.935	1.802	1.810	2.512	1.935	1.801	1.806	2.515	1.935	1.801	1.806
MPW1PBE	2.503	1.930	1.796	1.804	2.510	1.933	1.799	1.808	2.508	1.933	1.798	1.804	2.511	1.933	1.799	1.804
B1LYP	2.559	1.956	1.825	1.832	2.570	1.961	1.830	1.837	2.568	1.962	1.830	1.835	2.571	1.962	1.831	1.835
PBE1PBE	2.503	1.930	1.796	1.803	2.511	1.933	1.799	1.807	2.508	1.933	1.798	1.804	2.511	1.932	1.799	1.804
MPW1LYP	2.557	1.955	1.823	1.830	2.568	1.960	1.828	1.836	2.566	1.961	1.829	1.834	2.570	1.960	1.829	1.834
B98	2.539	1.947	1.813	1.820	2.547	1.952	1.817	1.825	2.545	1.951	1.817	1.821	2.548	1.951	1.817	1.821
X3LYP	2.553	1.953	1.819	1.825	2.563	1.958	1.824	1.831	2.561	1.958	1.824	1.829	2.565	1.958	1.825	1.829
B97-1	2.539	1.949	1.813	1.821	2.546	1.953	1.817	1.826	2.544	1.952	1.817	1.822	2.547	1.952	1.817	1.822
B97-2	2.521	1.939	1.805	1.811	2.530	1.942	1.809	1.815	2.526	1.942	1.808	1.811	2.529	1.941	1.808	1.811
MPW3PBE	2.513	1.935	1.798	1.805	2.520	1.938	1.801	1.809	2.517	1.938	1.801	1.806	2.521	1.938	1.801	1.806
B3LYP	2.557	1.955	1.820	1.826	2.567	1.960	1.825	1.832	2.565	1.961	1.825	1.830	2.568	1.961	1.825	1.829
B3PW91	2.517	1.937	1.800	1.807	2.525	1.941	1.804	1.812	2.522	1.940	1.803	1.808	2.525	1.940	1.804	1.808
B3P86	2.514	1.933	1.797	1.804	2.521	1.936	1.801	1.808	2.518	1.936	1.800	1.805	2.522	1.936	1.800	1.805
O3LYP	2.531	1.944	1.803	1.809	2.537	1.947	1.807	1.814	2.534	1.946	1.805	1.810	2.538	1.946	1.806	1.810
Hybrid Meta GGA																
M06-HF	2.661	2.031	1.942	1.927	2.678	2.066	1.945	1.933	2.675	2.048	1.941	1.926	2.679	2.052	1.948	1.921
M05-2X	2.554	1.947	1.845	1.847	2.567	1.955	1.849	1.852	2.565	1.954	1.849	1.845	2.567	1.954	1.849	1.845
M06-2X	2.575	1.965	1.864	1.873	2.592	1.972	1.868	1.881	2.589	1.972	1.867	1.871	2.592	1.972	1.868	1.871
MPWB1K	2.468	1.916	1.801	1.810	2.477	1.919	1.804	1.814	2.473	1.919	1.804	1.810	2.476	1.919	1.805	1.810
BB1K	2.471	1.919	1.802	1.810	2.480	1.921	1.805	1.814	2.476	1.921	1.805	1.811	2.479	1.921	1.806	1.810
M05	2.520	1.945	1.825	1.817	2.531	1.947	1.832	1.822	2.527	1.950	1.832	1.819	2.526	1.948	1.832	1.818
B1B95	2.487	1.929	1.802	1.809	2.495	1.931	1.806	1.813	2.491	1.931	1.805	1.810	2.494	1.931	1.806	1.810
M06	2.531	1.947	1.826	1.824	2.538	1.948	1.831	1.828	2.537	1.952	1.833	1.829	2.538	1.952	1.833	1.828
TPSSH	2.514	1.946	1.806	1.816	2.520	1.948	1.809	1.820	2.516	1.947	1.808	1.816	2.519	1.947	1.808	1.816
LC Hybrid GGA																
CAM-B3LYP	2.514	1.930	1.812	1.818	2.526	1.934	1.817	1.824	2.523	1.935	1.818	1.822	2.526	1.935	1.818	1.822
LC-ωPBE[b]	2.477	1.918	1.795	1.801	2.485	1.921	1.799	1.806	2.481	1.920	1.798	1.803				
experiment-1[a]	2.528	1.939	1.816	1.832	2.528	1.939	1.816	1.832	2.528	1.939	1.816	1.832	2.528	1.939	1.816	1.832

[a]Reference 21, crystal structure. [b]Refer to Table 1 footnote.

dx.doi.org/10.1021/ct4002398 | J. Chem. Theory Comput. XXXX, XXX, XXX−XXX

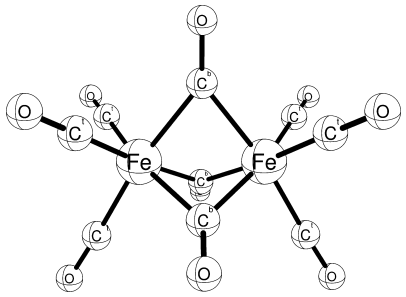

Figure 2. $Fe_2(CO)_9$ - D_{3h} symmetry.

much more pronounced for the M06-HF, M05-2X, M06-2X, and BHLYP functionals. The Co−Co bond distances predicted employing the DZP basis set are closer to the cc-pVTZ values compared to the cc-pVDZ and cc-pVQZ values, with differences ranging from 0.015 Å (for M06-2X) to less than 0.001 Å (for M06-L). For most functionals, the difference in DZP and cc-pVTZ results for the Co−Co bond length is between 0.005 and 0.003 Å. The Co−C bond distances are less dependent on the size of the correlation consistent basis sets but differ from DZP values from 0.008 to less than 0.001 Å. In spite of these differences in structural parameters between DZP an cc-pVXZ (X = D,T,Q) basis sets, one must note that the triple and quadruple-ζ quality basis sets do not give any more accurate bond lengths than the DZP basis set, compared to the experimental structures. Most functionals predict bond distances that are 0.02−0.04 Å away from the experimental values, regardless of the size or type of basis set employed.

Table 5. $Fe_2(CO)_9$ Bond Distances in Angstroms

	DZP			cc-pVDZ			cc-pVTZ			cc-pVQZ		
DFT method	Fe−Fe	Fe−C^b	Fe−C^t	Fe−Fe	Fe−C^b	Fe−C^t	Fe−Fe	Fe−C^b	Fe−C^t	Fe−Fe	Fe−C^b	Fe−C^t
GGA												
BLYP	2.566	2.034	1.841	2.575	2.040	1.849	2.572	2.040	1.846	2.575	2.040	1.846
BP86	2.519	2.006	1.819	2.526	2.010	1.826	2.522	2.010	1.822	2.524	2.010	1.822
B97-D	2.536	2.020	1.829	2.544	2.025	1.837	2.540	2.024	1.833	2.542	2.023	1.833
HCTH147	2.516	2.004	1.815	2.525	2.009	1.822	2.519	2.007	1.818	2.522	2.007	1.817
HCTH407	2.504	1.998	1.810	2.513	2.001	1.817	2.506	1.999	1.812	2.509	1.999	1.812
Meta GGA												
M06-L	2.515	2.010	1.827	2.521	2.011	1.834	2.512	2.009	1.827	2.514	2.010	1.826
VSXC	2.561	2.034	1.856	2.560	2.031	1.864	2.559	2.034	1.858	2.561	2.034	1.859
Hybrid GGA												
BHLYP	2.502	1.996	1.839	2.515	2.004	1.847	2.510	2.002	1.842	2.512	2.002	1.842
MPW1K	2.459	1.970	1.807	2.466	1.973	1.813	2.462	1.972	1.808	2.464	1.973	1.809
BHandH	2.473	1.978	1.819	2.484	1.985	1.827	2.478	1.983	1.822	2.481	1.984	1.822
MPW1PW91	2.479	1.981	1.807	2.485	1.984	1.814	2.481	1.984	1.810	2.484	1.984	1.810
MPW1PBE	2.475	1.979	1.805	2.481	1.982	1.812	2.477	1.981	1.807	2.480	1.981	1.807
B1LYP	2.528	2.009	1.833	2.539	2.016	1.841	2.535	2.015	1.837	2.537	2.015	1.838
PBE1PBE	2.473	1.978	1.805	2.480	1.981	1.811	2.476	1.980	1.807	2.478	1.981	1.807
MPW1LYP	2.526	2.008	1.832	2.537	2.014	1.840	2.533	2.013	1.837	2.535	2.014	1.837
B98	2.507	1.998	1.821	2.516	2.003	1.829	2.510	2.001	1.824	2.513	2.001	1.824
X3LYP	2.522	2.005	1.828	2.532	2.011	1.836	2.528	2.010	1.832	2.530	2.011	1.832
B97-1	2.507	2.000	1.822	2.515	2.004	1.830	2.510	2.002	1.824	2.512	2.002	1.825
B97-2	2.490	1.987	1.812	2.497	1.991	1.818	2.492	1.990	1.814	2.495	1.990	1.814
MPW3PBE	2.484	1.984	1.807	2.490	1.987	1.814	2.486	1.986	1.810	2.489	1.987	1.810
B3LYP	2.526	2.008	1.829	2.536	2.014	1.837	2.532	2.013	1.833	2.534	2.013	1.833
B3PW91	2.488	1.986	1.810	2.495	1.990	1.816	2.491	1.989	1.812	2.494	1.990	1.812
B3P86	2.483	1.982	1.807	2.490	1.986	1.813	2.486	1.985	1.809	2.489	1.985	1.809
O3LYP	2.495	1.991	1.810	2.501	1.994	1.817	2.496	1.992	1.812	2.499	1.993	1.812
Hybrid Meta GGA												
M06-HF	2.477	2.026	1.894	2.496	2.057	1.909	2.466	2.031	1.888	2.471	2.030	1.887
M05-2X	2.498	1.996	1.839	2.514	2.008	1.848	2.503	2.003	1.839	2.506	2.003	1.839
M06-2X	2.517	2.014	1.859	2.535	2.027	1.869	2.519	2.018	1.857	2.522	2.020	1.857
MPWB1K	2.449	1.965	1.809	2.455	1.967	1.816	2.451	1.966	1.812	2.454	1.967	1.812
BB1K	2.453	1.967	1.810	2.458	1.969	1.816	2.454	1.968	1.812	2.457	1.969	1.812
M05	2.479	1.988	1.821	2.485	1.987	1.829	2.480	1.989	1.824	2.480	1.987	1.823
B1B95	2.468	1.976	1.810	2.473	1.978	1.817	2.470	1.977	1.813	2.472	1.978	1.813
M06	2.497	1.993	1.827	2.501	1.994	1.835	2.503	1.998	1.833	2.504	1.998	1.833
TPSSH	2.499	1.996	1.819	2.503	1.998	1.826	2.499	1.997	1.821	2.502	1.998	1.821
LC Hybrid GGA												
CAM-B3LYP	2.485	1.980	1.821	2.495	1.985	1.829	2.491	1.985	1.826	2.494	1.985	1.826
LC-ωPBE[b]	2.452	1.963	1.804	2.457	1.964	1.812	2.454	1.965	1.807	2.457	1.965	1.808
experiment[a]	2.523	2.016	1.838	2.523	2.016	1.838	2.523	2.016	1.838	2.523	2.016	1.838

[a]Reference 72, crystal structure. [b]Refer to Table 1 footnote.

dx.doi.org/10.1021/ct4002398 | J. Chem. Theory Comput. XXXX, XXX, XXX−XXX

Table 6. $Mn_2(CO)_{10}$ Bond Distances in Angstroms

	DZP			cc-pVDZ			cc-pVTZ			cc-pVQZ		
DFT method	Mn−Mn	Mn−C^{ax}	Mn−C^{eq}	Mn−Mn	Mn−C^{ax}	Mn−C^{eq}	Mn−Mn	Mn−C^{ax}	Mn−C^{eq}	Mn−Mn	Mn−C^{ax}	Mn−C^{eq}
GGA												
BLYP	3.067	1.825	1.871	3.056	1.831	1.875	3.093	1.828	1.876	3.101	1.828	1.875
BP86	2.955	1.803	1.851	2.956	1.807	1.853	2.974	1.804	1.853	2.983	1.804	1.853
B97-D	2.988	1.812	1.855	2.989	1.817	1.857	3.004	1.814	1.858	3.011	1.813	1.858
HCTH147	3.037	1.792	1.845	3.031	1.796	1.847	3.061	1.793	1.848	3.071	1.792	1.847
HCTH407	3.046	1.786	1.841	3.031	1.796	1.847	3.075	1.786	1.844	3.084	1.786	1.843
Meta GGA												
M06-L	2.901	1.811	1.864	2.940	1.815	1.865	2.934	1.809	1.863	2.938	1.808	1.864
VSXC	2.973	1.841	1.883	3.005	1.849	1.884	2.994	1.843	1.885	3.008	1.843	1.885
Hybrid GGA												
BHLYP	3.013	1.832	1.881	3.033	1.841	1.888	3.045	1.834	1.886	3.050	1.833	1.885
MPW1K	2.903	1.796	1.848	2.925	1.801	1.851	2.927	1.796	1.850	2.935	1.795	1.850
BHandH	2.953	1.812	1.862	2.974	1.819	1.867	2.980	1.813	1.865	2.987	1.812	1.865
MPW1PW91	2.910	1.793	1.845	2.925	1.797	1.847	2.933	1.793	1.847	2.941	1.793	1.847
MPW1PBE	2.915	1.792	1.843	2.926	1.796	1.846	2.936	1.793	1.846	2.945	1.792	1.846
B1LYP	3.019	1.820	1.870	3.025	1.826	1.875	3.048	1.822	1.875	3.054	1.821	1.874
PBE1PBE	2.897	1.791	1.842	2.914	1.794	1.844	2.919	1.791	1.845	2.927	1.790	1.844
MPW1LYP	3.010	1.819	1.869	3.016	1.826	1.874	3.038	1.822	1.874	3.045	1.821	1.873
B98	2.968	1.807	1.858	2.977	1.812	1.861	2.989	1.808	1.860	2.997	1.807	1.861
X3LYP	2.998	1.814	1.864	3.004	1.820	1.868	3.025	1.816	1.868	3.032	1.815	1.868
B97-1	2.958	1.808	1.859	2.970	1.813	1.862	2.981	1.808	1.861	2.988	1.808	1.861
B97-2	2.958	1.794	1.848	2.969	1.797	1.850	2.982	1.794	1.850	2.991	1.793	1.849
MPW3PBE	2.903	1.791	1.843	2.917	1.794	1.845	2.924	1.791	1.845	2.933	1.790	1.844
B3LYP	3.007	1.814	1.864	3.011	1.820	1.869	3.034	1.817	1.869	3.041	1.816	1.868
B3PW91	2.928	1.794	1.846	2.939	1.798	1.848	2.949	1.794	1.848	2.958	1.794	1.848
B3P86	2.912	1.792	1.842	2.923	1.795	1.845	2.933	1.792	1.845	2.942	1.792	1.845
O3LYP	2.991	1.790	1.844	2.998	1.792	1.846	3.016	1.789	1.846	3.026	1.789	1.846
Hybrid Meta GGA												
M06-HF	2.953	1.892	1.927	2.982	1.916	1.944	2.958	1.883	1.922	2.974	1.877	1.916
M05-2X	2.948	1.822	1.877	2.964	1.831	1.884	2.963	1.820	1.879	2.973	1.818	1.878
M06-2X	2.950	1.841	1.898	2.982	1.853	1.907	2.970	1.837	1.899	2.979	1.834	1.898
MPWB1K	2.844	1.799	1.850	2.879	1.805	1.853	2.869	1.800	1.853	2.877	1.799	1.853
BB1K	2.848	1.799	1.850	2.882	1.804	1.853	2.872	1.799	1.853	2.882	1.798	1.853
M05	2.901	1.802	1.853	2.931	1.805	1.854	2.936	1.802	1.855	2.935	1.801	1.854
B1B95	2.851	1.795	1.847	2.881	1.800	1.849	2.873	1.796	1.850	2.886	1.796	1.850
M06	2.913	1.812	1.859	2.914	1.817	1.861	2.933	1.815	1.864	2.934	1.814	1.863
TPSSH	2.897	1.806	1.855	2.915	1.810	1.857	2.917	1.806	1.857	2.926	1.806	1.856
LC Hybrid GGA												
CAM-B3LYP	2.932	1.807	1.855	2.946	1.814	1.859	2.959	1.810	1.860	2.966	1.809	1.859
LC-ωPBE[d]	2.836	1.787	1.835	2.857	1.791	1.837	2.856	1.788	1.838	2.866	1.788	1.838
experiment-1[a]	2.895	1.820	1.859	2.895	1.820	1.859	2.895	1.820	1.859	2.895	1.820	1.859
experiment-2[b]	2.923	1.792	1.830	2.923	1.792	1.830	2.923	1.792	1.830	2.923	1.792	1.830
experiment-3[c]	2.977	1.803	1.873	2.977	1.803	1.873	2.977	1.803	1.873	2.977	1.803	1.873

[a]Reference 80, structure from electron density. [b]Reference 77, crystal structure. [c]Reference 81, gas phase electron diffraction. [d]Refer to Table 1 footnote.

E. $Fe_2(CO)_9$. The triply bridged structure with D_{3h} symmetry is the experimental structure of the $Fe_2(CO)_9$ dimer (see Figure 2). Even though the Fe−Fe bond distance in the dimer is only 2% larger than Fe−Fe bond distance in the bulk metal, theoretical studies[59,66−72] suggest the absence of a direct Fe−Fe bond in the triply bridged $Fe_2(CO)_9$. Jang et al. optimized the geometry of the dimer employing the DZP B3LYP method and determined the lengths of the Fe−Fe, Fe−C, and C−O bonds within 0.002, 0.01, and 0.005 Å of experiment.[38,72] Considering the fact that the experimental structures are solid state structures, bond distances in Table 5 determined for isolated $Fe_2(CO)_9$ molecule are reasonably close to experiment, especially for the BP86, HCTH-147, M06-L, B1LYP, MPW1LYP, X3LYP, B3LYP, and M06-2X functionals, which predict Fe−Fe, Fe−C^b, and Fe−C^t distances within 0.008, 0.011, and 0.019 Å. Increasing the basis set size from DZP to cc-pVQZ results in changes in bond lengths of less than 0.01 Å. In fact, the cc-pVTZ bond distances are very close to the DZP results; the Fe−Fe and Fe−C bond lengths are lengthened by not more than 0.003 Å upon changing the basis set from DZP to cc-pVTZ for as many as 21 functionals used in this study.

F. $Mn_2(CO)_{10}$. $Mn_2(CO)_{10}$ is a homoleptic binuclear carbonyl compound that was isolated later than the other 3d transition metal carbonyl compounds.[73−75] The molecule has D_{4d} symmetry (see Figure 3) with nonbridging carbonyls arranged in a staggered confirmation, and this structure was

dx.doi.org/10.1021/ct4002398 | J. Chem. Theory Comput. XXXX, XXX, XXX−XXX

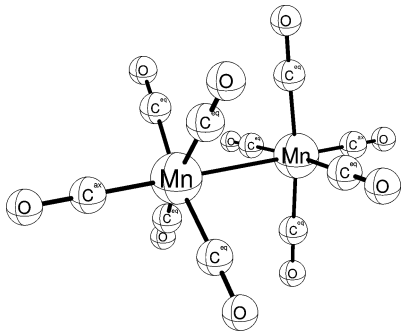

Figure 3. $Mn_2(CO)_{10}$ - D_{4d} symmetry.

found to be the global minimum.[76] The structure of $Mn_2(CO)_{10}$ with its undisputed direct Mn−Mn bond has been determined by a number of crystallographic[77−80] and electron diffraction studies.[81] The bond distances determined by various DFT methods in this study differ from the gas phase electron diffraction structures by 0.01 to 0.13 Å. The MPWB1K and BB1K methods give the largest differences in Mn−Mn bond distances, 0.133 to 0.129 Å, respectively, from the gas electron diffraction[81] value (2.977 Å). All the functionals correctly reproduce the relative lengths of the axial ($Mn-C_{ax}$) and equatorial ($Mn-C_{eq}$) bonds, with smaller absolute deviations from experiment for the $Mn-C_{ax}$ bond distance than $Mn-C_{eq}$. The Mn−Mn bond length increases by 0.015 to 0.034 Å from double-ζ (DZP) to the triple-ζ basis set. From the triple to the quadruple-ζ basis set, the Mn−Mn distance increases further, by 0.006 to 0.015 Å. This suggests a significant basis set dependence of the Mn−Mn bond distance. Despite this, the DZP basis predictions for r_e(Mn−Mn) are closer to experiment than are the cc-pVQZ results.

With the large basis sets cc-pVTZ and cc-pVQZ, the Mn−Mn bond lengths deviate from the electron diffraction experiment by 0.12 Å (for the BLYP functional) to less than 0.005 Å (for BP86, BHandH, B97-1, B97-2, M06-HF, M05-2X, and M06-2X). Mean absolute deviations from the experiment are 0.05 Å for both the cc-pVTZ and cc-pVQZ basis. In contrast to the performance of the M06-HF, M05-2X, and M06-2X methods for predicting other M−M bonds distances, the Fe−Fe bond distances predicted by the three methods are very close to experiment, in fact, closer than those predicted by most of the functionals. The M06-HF, M05-2X, and M06-2X methods with the cc-pVQZ basis set predict Fe−Fe distances within 0.003, 0.004, and 0.002 Å, respectively, of experiment.

4. CONCLUSIONS

Structures of $Ni(CO)_4$, $Fe(CO)_5$, $Cr(CO)_6$, $Co_2(CO)_8$, $Fe_2(CO)_9$, and $Mn_2(CO)_{10}$ have been optimized in this study, employing the double, triple, and quadruple-ζ correlation consistent basis sets (cc-pVXZ) and the Hood-Pitzer extended double-ζ polarization (DZP) basis set. Comparison of M−M and M−L bond distances as a function of basis set size for 35 functionals shows that the DZP basis set generally predicts structural parameters on par with the correlation consistent triple and quadruple-ζ basis sets. The Mn−Mn bond distance shows more basis set dependence than the other two M−M bond lengths. Overall, the M06-L method predicts M−M and M−L bond distances in better agreement with experimental values, even with a relatively small basis set like the Hood-Pitzer DZP basis set. The DZP basis set, surprisingly, predicts structural parameters with reasonable accuracy and greatly reduces the computational cost of optimizing the structures of larger systems. In our study, the DZP M06-L method bests the other methods in terms of accuracy and computational cost.

Large basis sets such as cc-pVQZ can be applied to small organometallic systems such as those studied here. However, when one considers large transition metal systems (e.g., 1000 atoms), recently developed linear scaling methods[82] become necessary for *ab initio* computations. For such large systems, the powerful advantages of linear scaling methods are severely compromised when extended basis sets such as cc-pVQZ are employed. Linear scaling methods demand that basis functions be local, and this is not the case with the more diffuse basis functions that exist in the quadruple-ζ sets. Thus the general reliability of smaller basis sets, such as the Hood-Pitzer sets, is important for the future of quantum chemistry.

■ ASSOCIATED CONTENT

Supporting Information

Tables S1a−S6a compare M−M and M−L bond distances with experiment. Tables S1b−S6b compare bond distances from cc-pVXZ (X = D,T,Q) basis sets with DZP results. This material is available free of charge via the Internet at http://pubs.acs.org.

■ AUTHOR INFORMATION

Corresponding Author

*E-mail: qc@uga.edu.

Notes

The authors declare no competing financial interest.

■ ACKNOWLEDGMENTS

This research was supported by the National Science Foundation (NSF), Grant No. CHE-1054286.

■ REFERENCES

(1) Ziegler, T. *Can. J. Chem.* **1995**, *73*, 743−761.
(2) Ignatyev, I. S.; Schaefer, H. F.; King, R. B.; Brown, S. T. *J. Am. Chem. Soc.* **2000**, *122*, 1989−1994.
(3) Schultz, N. E.; Zhao, Y.; Truhlar, D. G. *J. Phys. Chem. A* **2005**, *109*, 11127−11143.
(4) Schultz, N. E.; Zhao, Y.; Truhlar, D. G. *J. Phys. Chem. A* **2005**, *109*, 4388−4403.
(5) Boese, A. D.; Martin, J. M. L.; Handy, N. C. *J. Chem. Phys.* **2003**, *119*, 3005−3014.
(6) Jensen, F. *J. Chem. Phys.* **2002**, *116*, 7372−7379.
(7) Wang, N. X.; Wilson, A. K. *J. Chem. Phys.* **2004**, *121*, 7632−7646.
(8) Tekarli, S. M.; Drummond, M. L.; Williams, T. G.; Cundari, T. R.; Wilson, A. K. *J. Phys. Chem. A* **2009**, *113*, 8607−8614.
(9) Jensen, F. *J. Chem. Phys.* **2013**, *138*, 14107.
(10) Dunning, T. H. *J. Chem. Phys.* **1989**, *90*, 1007−1023.
(11) Balabanov, N. B.; Peterson, K. A. *J. Chem. Phys.* **2005**, *123*, 064107.
(12) Balabanov, N. B.; Peterson, K. A. *J. Chem. Phys.* **2006**, *125*, 074110.
(13) Dunning, T. H. *J. Chem. Phys.* **1970**, *53*, 2823−2833.
(14) Huzinaga, S. *J. Chem. Phys.* **1965**, *43*, 1293−1302.
(15) Wachters, A. J. H. *J. Chem. Phys.* **1970**, *52*, 1033−1036.
(16) Hood, D. M.; Pitzer, R. M.; Schaefer, H. F. *J. Chem. Phys.* **1979**, *71*, 705−712.
(17) Valiev, M.; Bylaska, E. J.; Govind, N.; Kowalski, K.; Straatsma, T. P.; van Dam, H. J. J.; Wang, D.; Nieplocha, J.; Apra, E.; Windus, T. L.; de Jong, W. A. *Comput. Phys. Commun.* **2010**, *181*, 1477−1489.
(18) Papas, B. N.; Schaefer, H. F. *J. Mol. Struct.* **2006**, *768*, 175−181.
(19) Mura, M. E.; Knowles, P. J. *J. Chem. Phys.* **1996**, *104*, 9848−9858.

(20) Lebedev, V. I.; Laikov, D. N. *Russ. Acad. Sci. Dokl. Math.* **1999**, *59*, 477−481.
(21) Leung, P. C.; Coppens, P. *Acta Crystallogr.* **1983**, *B39*, 535−542.
(22) Ladell, J.; Post, B.; Fankuchen, I. *Acta Crystallogr.* **1952**, *5*, 795−800.
(23) Braga, D.; Grepioni, F.; Orpen, A. G. *Organometallics* **1993**, *12*, 1481−1483.
(24) Hedberg, L.; Iijima, T.; Hedberg, K. *J. Chem. Phys.* **1979**, *70*, 3224−3229.
(25) Mitin, A. V.; Baker, J.; Pulay, P. *J. Chem. Phys.* **2003**, *118*, 7775−7782.
(26) Bolshakov, V. I.; Rossikhin, V. V.; Voronkov, E. U.; Okovytyy, S. I.; Leszczynski, J. *J. Comput. Chem.* **2007**, *28*, 778−782.
(27) Calaminici, P.; Janetzko, F.; Köster, A. M.; Mejia-Olvera, R.; Zuniga-Gutierrez, B. *J. Chem. Phys.* **2007**, *126*, 044108.
(28) Davis, M. I.; Hanson, H. P. *J. Phys. Chem.* **1965**, *69*, 3405−3410.
(29) Hanson, H. P. *J. Phys. Chem.* **1967**, *71*, 775−777.
(30) Beagley, B.; Cruickshank, D. W. J.; Pinder, P. M.; Robiette, A. G.; Sheldrick, G. M. *Acta Crystallogr., Sect. B* **1969**, *25*, 737.
(31) Almenningen, A.; Haaland, A.; Wahl, K. *Acta Chem. Scand.* **1969**, *23*, 2245−2252.
(32) Beagley, B.; Schmidling, D. G. *J. Mol. Struct.* **1974**, *22*, 466−468.
(33) McClelland, B. W.; Robiette, A. G.; Hedberg, L.; Hedberg, K. *Inorg. Chem.* **2001**, *40*, 1358−1362.
(34) Lüthi, H. P.; Siegbahn, P. E. M.; Almlöf, J. *J. Phys. Chem.* **1985**, *89*, 2156−2161.
(35) Jonas, V.; Thiel, W. *J. Chem. Phys.* **1995**, *102*, 8474−8484.
(36) Bérces, A.; Ziegler, T. *J. Phys. Chem.* **1995**, *99*, 11417−11423.
(37) Li, J.; Schreckenbach, G.; Ziegler, T. *J. Am. Chem. Soc.* **1995**, *117*, 486−494.
(38) Jang, J. H.; Lee, J. G.; Lee, H.; Xie, Y.; Schaefer, H. F. *J. Phys. Chem. A* **1998**, *102*, 5298−5304.
(39) González-Blanco, O.; Branchadell, V. *J. Chem. Phys.* **1999**, *110*, 778−783.
(40) Ehlers, A. W.; Frenking, G. *J. Am. Chem. Soc.* **1994**, *116*, 1514−1520.
(41) Fan, L. Y.; Ziegler, T. *J. Chem. Phys.* **1991**, *95*, 7401−7408.
(42) Fournier, R. *J. Chem. Phys.* **1993**, *99*, 1801−1815.
(43) Farrugia, L. J.; Evans, C. *J. Phys. Chem. A* **2005**, *109*, 8834−8848.
(44) Ishikawa, Y.; Kawakami, K. *J. Phys. Chem. A* **2007**, *111*, 9940−9944.
(45) Delley, B.; Wrinn, M.; Lüthi, H. P. *J. Chem. Phys.* **1994**, *100*, 5785−5791.
(46) Li, J.; Schreckenbach, G.; Ziegler, T. *J. Phys. Chem.* **1994**, *98*, 4838−4841.
(47) Jost, A.; Rees, B.; Yelon, W. B. *Acta Crystallogr.* **1975**, *B31*, 2649−2658.
(48) Whitaker, A.; Jeffery, J. W. *Acta Crystallogr.* **1967**, *23*, 977−984.
(49) Rees, B.; Mitschler, A. *J. Am. Chem. Soc.* **1976**, *98*, 7918−7924.
(50) Koelle, U. In *Encyclopedia of Inorganic Chemistry*; King, R., Ed.; Wiley: Chichester, England, 1994; pp 773−747.
(51) Bor, G.; Noack, K. *J. Organomet. Chem.* **1974**, *64*, 367−372.
(52) Bor, G.; Dietler, U. K.; Noack, K. *J. Chem. Soc., Chem. Commun.* **1976**, 914−916.
(53) Onaka, S.; Shriver, D. F. *Inorg. Chem.* **1976**, *15*, 915−918.
(54) Kenny, J. P.; King, R. B.; Schaefer, H. F. *Inorg. Chem.* **2001**, *40*, 900−911.
(55) Sumner, G. G.; Klug, H. P.; Alexander, L. E. *Acta Crystallogr.* **1964**, *17*, 732−742.
(56) Braga, D.; Grepioni, F.; Sabatino, P.; Gavezzotti, A. *J. Chem. Soc., Dalton Trans.* **1992**, 1185−1191.
(57) Thorn, D. L. *Inorg. Chem.* **1978**, *17*, 126−140.
(58) Dedieu, A.; Albright, T. A.; Hoffmann, R. *J. Am. Chem. Soc.* **1979**, *101*, 3141−3151.
(59) Heijser, W.; Baerends, E. J.; Ros, P. *Faraday Symp. Chem. Soc.* **1980**, *14*, 211−234.
(60) Bellagamba, V.; Ercoli, R.; Gamba, A.; Suffritti, G. B. *J. Organomet. Chem.* **1980**, *190*, 381−392.
(61) Low, A. A.; Kunze, K. L.; MacDougall, P. J.; Hall, M. B. *Inorg. Chem.* **1991**, *30*, 1079−1086.
(62) Folga, E.; Ziegler, T. *J. Am. Chem. Soc.* **1993**, *115*, 5169−5176.
(63) Uffing, C.; Ecker, A.; Köppe, R.; Schnöckel, H. *Organometallics* **1998**, *17*, 2373−2375.
(64) Barckholtz, T. A.; Bursten, B. E. *J. Am. Chem. Soc.* **1998**, *120*, 1926−1927.
(65) Barckholtz, T. A.; Bursten, B. E. *J. Organomet. Chem.* **2000**, *596*, 212−220.
(66) Summerville, R. H.; Hoffmann, R. *J. Am. Chem. Soc.* **1979**, *98*, 7240−7254.
(67) Bauschlicher, C. W. *J. Chem. Phys.* **1986**, *84*, 872−875.
(68) Rosa, A.; Baerends, E. J. *New. J. Chem.* **1991**, *15*, 815−829.
(69) Bo, C.; Sarasa, J.-P.; Poblet, J.-M. *J. Phys. Chem.* **1993**, *97*, 6362−6366.
(70) Reinhold, J.; Hunstock, E. *New J. Chem.* **1994**, *18*, 465−471.
(71) Jacobsen, H.; Ziegler, T. *J. Am. Chem. Soc.* **1996**, *118*, 4631−4635.
(72) Cotton, F. A.; Troup, J. M. *J. Chem. Soc., Dalton Trans.* **1974**, 800−802.
(73) Brimm, E. O.; Lynch, M. A.; Sesny, W. J. *J. Am. Chem. Soc.* **1954**, *76*, 3831−3835.
(74) Closson, R. D.; Buzbee, L. R.; Ecke, G. C. *J. Am. Chem. Soc.* **1958**, *80*, 6167−6170.
(75) Podall, H. E.; Dunn, J. H.; Shapiro, H. J. *J. Am. Chem. Soc.* **1960**, *82*, 1325−1330.
(76) Xie, Y.; Jang, J. H.; King, R. B.; Schaefer, H. F. *Inorg. Chem.* **2003**, *42*, 5219−5230.
(77) Dahl, L. F.; Rundle, R. E. *Acta Crystallogr.* **1963**, *16*, 419−426.
(78) Dahl, L. F.; Ishishi, E.; Rundle, R. E. *J. Chem. Phys.* **1957**, *26*, 1750−1751.
(79) Churchill, M. R.; Amoh, K. N.; Wasserman, H. J. *Inorg. Chem.* **1981**, *20*, 1609−1611.
(80) Martin, M.; Rees, B.; Mitschler, A. *Acta Crystallogr.* **1982**, *B38*, 6−15.
(81) Almennin, A.; Jacobsen, G. G.; Seip, H. M. *Acta Chem. Scand.* **1969**, *23*, 685−686.
(82) Maurer, S. A.; Lambrecht, D. S.; Flaig, D.; Ochsenfeld, C. *J. Chem. Phys.* **2012**, *136*, 144107.
(83) http://www.nwchem-sw.org/index.php/Release61:Density_Functional_Theory_for_Molecules (accessed May 19, 2013).